TERM

ORIGINAL ARTICLE

Generation of Scalable Hepatic Micro-Tissues as a Platform for Toxicological Studies

Sara Darakhshan[1] · Ali Bidmeshki Pour[1] · Reza Kowsari-Esfahan[2] ·
Massoud Vosough[3] · Leila Montazeri[2] · Mohammad Hossein Ghanian[2] ·
Hossein Baharvand[3,4] · Abbas Piryaei[5,6]

Abstract

BACKGROUND: Currently, there is an urgent need for scalable and reliable *in vitro* models to assess the effects of therapeutic entities on the human liver. Hepatoma cell lines, including Huh-7, show weakly resemblance to human hepatocytes, limiting their significance in toxicity studies. Co-culture of hepatic cells with non-parenchymal cells, and the presence of extracellular matrix have been shown to influence the biological behavior of hepatocytes. The aim of this study was to generate the scalable and functional hepatic micro-tissues (HMTs).

METHODS: The size-controllable HMTs were generated through co-culturing of Huh-7 cells by mesenchymal stem cells and human umbilical vein endothelial cells in a composite hydrogel of liver-derived extracellular matrix and alginate, using an air-driven droplet generator.

RESULTS: The generated HMTs were functional throughout a culture period of 28 days, as assessed by monitoring glycogen storage, uptake of low-density lipoprotein and indocyanine green. The HMTs also showed increased secretion levels of albumin, alpha-1-antitrypsin, and fibrinogen, and production of urea. Evaluating the expression of genes involved in hepatic-specific and drug metabolism functions indicated a significant improvement in HMTs compared to two-dimensional (2D) culture of Huh-7 cells. Moreover, in drug testing assessments, HMTs showed higher sensitivity to hepatotoxins compared to 2D cultured Huh-7 cells. Furthermore, induction and inhibition potency of cytochrome P450 enzymes confirmed that the HMTs can be used for *in vitro* drug screening.

CONCLUSION: Overall, we developed a simple and scalable method for generation of liver micro-tissues, using Huh-7, with improved hepatic-specific functionality, which may represent a biologically relevant platform for drug studies.

Keywords Hepatic micro-tissue · Bioengineering · Toxicology · Hepatocyte functionality · Extracellular matrix

✉ Ali Bidmeshki Pour
abidmeshki@razi.ac.ir

✉ Hossein Baharvand
Baharvand@royaninstitute.org

✉ Abbas Piryaei
piryae@sbmu.ac.ir

[1] Department of Biology, Faculty of Science, Razi University, Kermanshah 6714414971, Iran

[2] Department of Cell Engineering, Cell Science Research Center, Royan Institute for Stem Cell Biology and Technology, ACECR, Tehran, Iran

[3] Department of Stem Cells and Developmental Biology, Cell Science Research Center, Royan Institute for Stem Cell Biology and Technology, ACECR, P.O. Box: 16635-148, Tehran, Iran

[4] Department of Developmental Biology, University of Science and Culture, Tehran, Iran

1 Introduction

Since the liver is the main site for metabolism of xenobiotics, the majority of drugs may have toxic effects on this organ. Drug-induced liver injury (DILI) is a main cause of acute and fulminant liver failure, also leading to a halt in the way of development and regulatory approval of new drugs [1, 2]. Safety-related issues are mainly due to the inefficiency of existing practical scalable and reliable models utilized for toxicity assessment. Although traditional methods used for predicting human response to drugs, mainly including *in vivo* or 2D *in vitro* cell-based assays, have resulted in a vast number of discoveries, the processes are fraught with difficulties [3]. Application of laboratory animals largely fail to reveal important signs of toxicity in human because of numerous inter-species differences [4]. As a result, to obtain credible data, human-specific responses to drugs should be studied in human cell-based platforms [5]. Primary human hepatocytes (PHHs), cultured as a monolayer or sandwich, are the cell sources preferred for toxicological evaluations [6, 7]. However, rapid loss of function, expensive *ex vivo* maintenance, and inter-donor variability are challenges accompanying the use of PHHs [8]. Hepatocyte-like cells (HLCs), derived from human pluripotent stem cells (hPSCs), as an alternative, could provide an unlimited supply of cells for drug screening and precision medicine [9, 10]. However, the production of HLCs is an expensive process, and obtained cells show characteristics similar to fetal hepatocytes with low drug metabolism capacity [11, 12]. Hepatoma cell lines, as another alternative source, can be considered as a suitable option for *in vitro* drug testing since they are relatively easy to store and maintain and provide more stable and affordable hepatocytes. However, these cell lines typically demonstrate low functionality and a declined metabolism compared to PHHs [5].

Traditional *in vitro* cell-based models are of limited value because the cells require complexity of the microenvironment to function and perform as they would *in vivo* [3]. PHHs rapidly lose their phenotype and function in 2D cultures *ex vivo* [13]. Therefore, widely used 2D cultured cell lines are inherently flawed by reduced liver tissue-specific functions [14]. To overcome these limitations, more sophisticated approaches are needed to better recapitulate a liver-specific microenvironment [13]. Three-

dimensional (3D) cell cultures are currently the most accepted approach for functional *in vitro* liver models. Multicellular spheroids, micro-tissues, or organoids are 3D clusters of cells with enhanced cell–cell contacts that can be produced using a number of methods, with or without scaffolds [15–19]. When cultured in spheroids, PHHs retained morphology, viability, and functions for five weeks, and they can model some liver diseases or be used for long-term DILI [19]. Several studies showed that some hepatoma cell lines, including HepG2, C3A, and Huh-7 cultured in 3D, displayed enhanced hepatic functionality compared to 2D cultures [15, 18–21]. HepG2 cells cultured using Matrigel™ in 3D fashion re-acquired lost functions of hepatocyte, such as glycogen storage, and bile canaliculi-like structures formation [18]. Furthermore, HepG2 spheroids showed a considerable improvement in albumin (ALB) secretion and metabolic activity as well as upregulation of phase I and II drug-metabolizing enzymes when compared with 2D cultures [15]. Huh-7 cells when cultured in spheroids showed enhanced expression of markers related to apical and basolateral polarization, cell adhesion, and tight junctions [22]. While the majority of *in vitro* liver models focus on hepatocyte source, there is evidence that suggests the presence of supportive cells in these models can produce more organotypic culture systems, with enhanced hepatic functions [19, 23, 24]. In a study carried out using co-culture of immortalized Upcyte® cells, comprised of PHHs, mesenchymal stem cells (MSCs) and liver sinusoidal endothelial cells (LSECs) on Matrigel™, liver organoid-like structures were obtained and remained functional for 10 days [24].

In addition to non-parenchymal cells, employing extracellular matrix (ECM) components can recapitulate native tissue microenvironment and support HLCs differentiation or hepatocyte survival, proliferation, and functionality [15, 16, 25–27]. Collagen type I and fibronectin, by distinct roles, promote liver-specific gene expression and ALB secretion of Huh-7.5 cells cultured in a 3D system [16]. In a liver-on-a-chip platform developed by Bhise et al., HepG2/C3A spheroids encapsulated by photocrosslinkable gelatin methacryloyl hydrogel remained functional for 30 days [15]. Our previous study showed that liver organoids produced via self-organization of Huh-7 in combination with human MSCs and endothelial cells in a liver-derived ECM hydrogel significantly enhanced the functionality of the hepatoma cell line, especially in terms of ALB secretion, urea production, and cytochrome P450 (CYP) enzymes activity and inducibility [28]. In the present study, we developed an air-driven microencapsulation system to generate hepatic micro-tissues (HMTs) in a size-controlled, reproducible, and scalable manner. The bioengineered HMTs were proven as an *in vitro* liver model which showed appropriate hepatic-specific functionality

5 Department of Biology and Anatomical Sciences, School of Medicine, Shahid Beheshti University of Medical Sciences, P.O. Box: 19395-4719, Tehran, Iran

6 Department of Tissue Engineering and Applied Cell Sciences, School of Advanced Technologies in Medicine, Shahid Beheshti University of Medical Sciences, Tehran, Iran

and relevant sensitivity for drug testing and were responsive for toxicological experiments.

2 Materials and methods

2.1 Cell culture

Huh-7 cells (kindly provided by Professor Andreas K. Nussler) were cultured and expanded in high-glucose Dulbecco's modified Eagle's medium (DMEM, Gibco, Gaithersburg, MD, USA, 11995-040). Full characterized human embryonic stem cell-derived mesenchymal stem cells (hES-MSCs), which were previously established from hES-RH5 cell line [29], obtained from Royan Stem Cell Bank (Tehran, Iran), were expanded in α-minimum essential *medium (*α-MEM, Sigma-Aldrich, St. Louis, MO, USA, M2279), and used at passages 3–5. Human umbilical vein endothelial cells (HUVECs) were isolated from umbilical cord of healthy newborns, after obtaining informed consent from their parents, using 1% collagenase (Gibco, 17104-019), maintained in endothelial growth medium (Royan Endothelial Cell Medium), and used at passages 1–3. All culture media were supplemented with 10% fetal bovine serum (FBS, Gibco, 16140-071), 1% penicillin/streptomycin (Pen/Strep, Gibco, 15070-063), 1% L-glutamine (Gibco, 25030-024), and MEM non-essential amino acids (Gibco, 11140-035). The medium refreshment was done every other day.

2.2 Preparation of hydrogels

Liver-derived ECM hydrogel (LEMgel) was prepared and characterized according to our previously reported protocol with minor modifications [28]. Briefly, we used 1% sodium dodecyl sulfate (SDS, Sigma-Aldrich, 436,143) and 1% Triton X-100 (Merck, Burlington, MA, USA, 108,643) to decellularize sheep liver tissue and achieve LEM. Then, the lyophilized LEM was milled using CHRIST lyophilizer (Alpha 1–2 LD plus, Osterode am Harz, Germany), sterilized via UV irradiation, and digested at a concentration of 6 mg/ml, using 1% (w/v) pepsin (Merck, P6887) and 0.5 M acetic acid. The stock solution of 6 mg/ml LEMgel was kept at 4 °C until further use.

Alginate (Alginic acid sodium salt, Sigma-Aldrich, 180,947) was dissolved to prepare a 2% concentration in distilled water and stirred overnight. To achieve an appropriate hydrogel mixture, named composite, equal volumes of 6 mg/ml LEMgel and 2% alginate were mixed to obtain a homogenous solution with a final concentration of 3 mg/ml and 1% for LEMgel and alginate, respectively (Fig S1A).

2.3 Characterization of the composite hydrogel

2.3.1 Scanning electron microscopy

To evaluate the microstructure of the composite hydrogel, a cylindrical sample was fixed using 4% glutaraldehyde in cacodylate buffer for 2 h at room temperature. After lyophilization, a fractured surface of the sample was gold-coated using ion sputtering and evaluated using a Jeol field emission scanning electron microscope (JSM-7400 M, Tokyo, Japan).

2.3.2 Rheometry

To compare the stiffness of the single-component and the composite hydrogels, the samples of 1% alginate, 3 mg/ml LEMgel, and the mixture of 1% alginate and 3 mg/ml LEMgel were prepared into a cylindrical shape (18 mm in diameter and 3 mm in height). Rheological characterization was performed using a rheometer (Anton-Paar, Graz, Austria, MCR 300) under strain-controlled conditions at 37 °C. The analysis was performed for 10 min at 0.1% strain over a range of frequencies from 0.1 to 100 Hz.

2.4 Hepatic micro-tissue formation

The HMTs were generated using an extrusion method adapted in our laboratory, as schematically illustrated in Fig. 1A. A homogeneous solution of the composite hydrogel was prepared, mixing neutralized LEMgel and alginate solutions at a final concentration of 3 mg/ml and 1% (w/v), respectively. An optimized cell ratios from Huh-7, HUVECs, and MSCs, at 3:2:1, respectively, was selected according to our previously published data [28]. A suspension of total 8×10^6 cells was prepared and centrifuged. Then, 1 ml of the composite was added to the cell pellet and gently mixed to ensure a homogeneous cell-laden suspension was made. The resultant cell-laden composite hydrogel was loaded in a 5-ml syringe with a 24G blunt needle and injected using a syringe pump (Harvard Apparatus, Holliston, MA, USA, PHD ULTRA™). The size of HMTs was tuned by controlling air and fluid flow rate to achieve the HMTs with 300, 500, or 700 μm in diameter. The generated HMTs fell into a gelling bath containing 100 mM calcium chloride at 37 °C. Finally, the generated HMTs were rinsed by the basal medium (DMEM) and cultured in complete mixed medium (CMM) for 28 days. According to the cells ratios, the CMM consisted of DMEM, α-MEM, and EGM media at a ratio of 3:2:1, respectively, and was supplemented with 10% FBS, 1% Pen/Strep, 1% L-glutamine, and 1% MEM non-essential amino acids. From the initial culture day up to day 7, the medium exchange was done every other day,
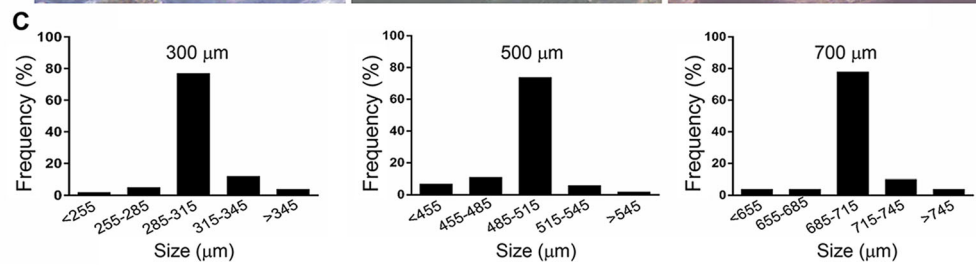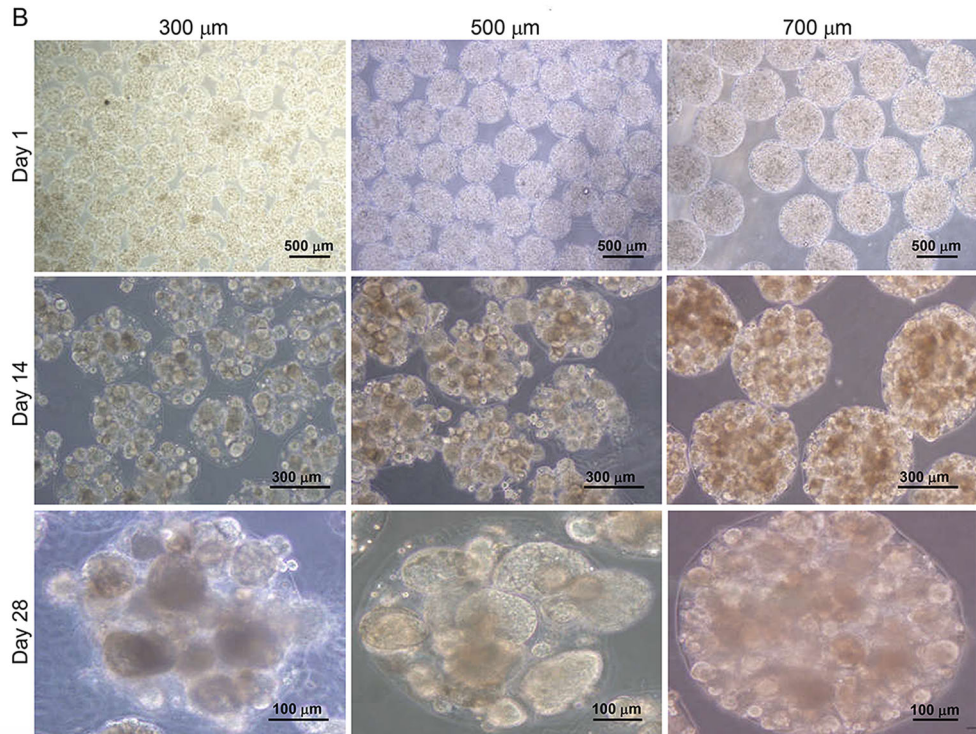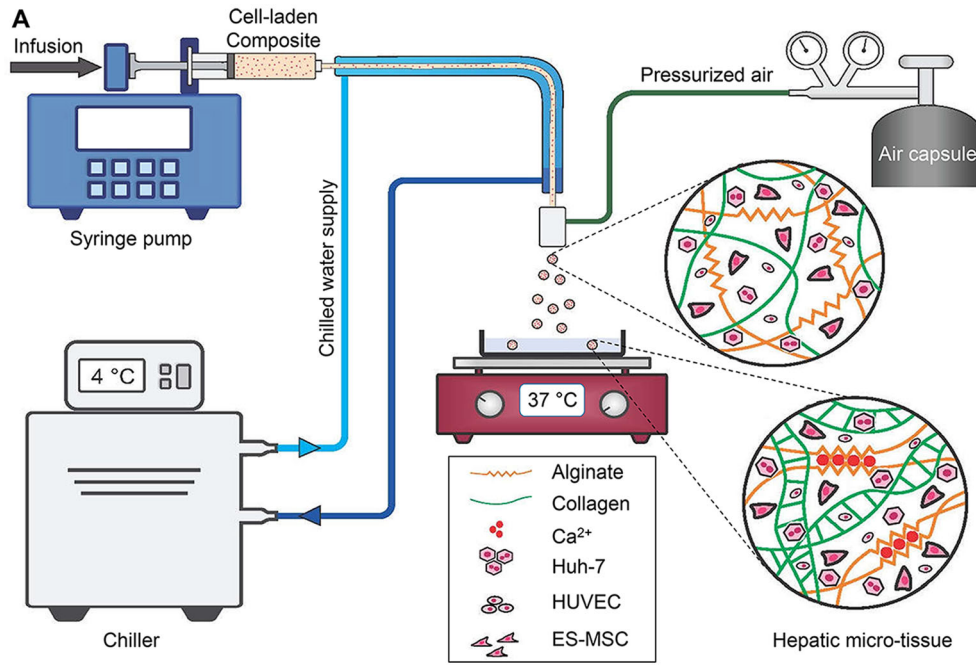
◄**Fig. 1** Hepatic micro-tissue bioengineering and characterization. **A** Schematic illustration of size-controlled HMTs formation using an air-driven droplet generator loaded with cell laden composite containing Huh-7, HUVECs and MSCs at a total density of 8×10^6 cells/ml. Upon entrance of the droplets into gelling bath, the fast gelation of alginate resulted in formation of round HMTs. **B** Phase-contrast micrographs of the generated HMTs showed that on day 1, the single cells were homogeneously distributed in the micro-tissues, while on day 28, a number of cell aggregates were formed inside the HMTs. **C** Size distribution evaluation showed that the extrusion method could efficiently generate HMTs with homogenous diameter

while from day 7 to 28, the medium refreshment was done daily.

2.5 Hepatic micro-tissue size distribution and cell proliferation

To evaluate the size distribution of generated HMTs and their possible variations during the culture period, the diameter of 100 HMTs was measured for each group using DP2-BSW software associated with a phase-contrast microscope (Olympus, IX71, Tokyo, Japan) on days 1, 14, and 28. Furthermore, to investigate the HMTs growth via cell proliferation, cell number per HMT was counted on days 1, 14, and 28, using an effective method [30], and the results were reported as fold changes relative to that of day 1. To do this, all cells existing in a certain number of HMTs were extracted by a two-step process, using 1% sodium citrate at first, in order to breakdown of alginate–calcium interactions. Next, we applied 1 mg/ml collagenase IV solution to degrade the crosslinks between collagen fibers. Finally, cell number was determined using trypan blue, and the counting was repeated three times for three independent experiments.

2.6 Live/dead assay

Cell viability of the HMTs was evaluated using LIVE/DEAD Viability/Cytotoxicity Kit (Invitrogen, L3224, Carlsbad, CA, USA) on day 28 according to instructions provided by the manufacturer. Briefly, the HMTs were washed with PBS and stained using calcein-AM (2 μM) and ethidium homodimer (4 μM) for 30 min at room temperature. Micrographs were acquired using an inverted fluorescence microscope (Olympus, IX71).

2.7 Gene expression analysis

Total RNA was extracted using RNeasy Mini Kit (QIA-GEN, 74106, Venlo, Netherlands), according to the manufacturer instructions. The quality of the total RNA was controlled using 1% agarose gel and a spectrophotometer (Biochrom WPA Biowave II, Cambridge, UK). Next, 2 g of RNA was subjected to reverse transcription using PrimeScript^{TM} RT reagent Kit (Takara Bio Inc., Kusatsu-Shi, Japan, RR037A). Quantitative RT-polymerase chine reaction (qRT-PCR) was performed using SYBR® Premix Ex Taq^{TM} II (Takara Bio Inc., RR820A) on the StepOnePlus Real-Time PCR system (Applied Biosystems StepOne instrument), and the level of target genes expression was normalized against glyceraldehyde 3-phosphate dehydrogenase (GAPDH). Monolayer Huh-7 cells and human adult liver tissue were considered as control groups. The normal liver tissue was collected from margin of resected tumor of a male 41-years old patient, who underwent partial hepatectomy as part of the treatment regime, after obtaining informed consent, at Imam Khomeini Hospital Complex. The qRT-PCR was performed in duplicate for three independent experiments. The primer sequences are listed in Table S1.

2.8 Liver-specific protein secretion and urea production assays

Enzyme-linked immunosorbent assay (ELISA) was performed to assess the secretion of three liver-specific proteins, albumin (ALB, Bethyl Laboratories, Montgomery, TX, USA, E88-129), alpha-1 antitrypsin (A1AT, GenWay Biotech, San Diego, CA, USA, GWB-5428A0), and fibrinogen (GenWay Biotech, San Diego, CA, USA, 40-288-22856), according to the manufacturer's instructions. Urea level in the culture media was measured using a colorimetric assay kit (Pars Azmun, assay kit (Pars Azmun, Tehran, Iran, 130400) according to the manufacturer's instruction. The media were collected on days 1, 7, 14, 21, and 28, following 24-h incubation of a certain number of HMTs that were initially generated from 2×10^6 cells, which included 10^6 Huh-7 cells. The assays were performed in duplicates for three independent experiments.

2.9 DiI-Ac-low-density lipoprotein (LDL) uptake

The HMTs were incubated with 10 μg/ml DiI-Ac-LDL solution (Biomedical Technologies Inc., Shanghai, China, BT-902) for 4 h at 37 °C on day 28. Then, the HMTs were thoroughly washed and imaged using fluorescence microscopy.

2.10 Indocyanine green (ICG) uptake/release

On day 28, the HMTs were incubated for 1 h with freshly prepared ICG solution (CardioGreen; Sigma-Aldrich, 12633) at the concentration of 1 mg/ml. Following rinsing, ICG uptake was evaluated using a phase-contrast microscope. Next, ICG release was evaluated after 16 h incubation of the HMTs in ICG-free culture medium.

2.11 Histology and immunofluorescence

To evaluate the structure and *in situ* liver-specific protein expression, some of the HMTs were harvested on day 28. The samples were fixed using 4% paraformaldehyde (PFA) and embedded in paraffin, and 6-μm sections underwent hematoxylin and eosin (H&E), Periodic acid-Schiff (PAS) or immunofluorescence staining. For immunostaining, the sections were permeabilized with 1% Triton X-100 in PBS, and exposed to 10% related sera. Then, the sections were incubated with primary antibodies against human Ki-67 (Abcam, ab15580, Cambridge, UK, 1:100), human albumin (Bethyl A80-229A, 1:200), human CYP3A4 (Santa Cruz, Dallas, TX, USA, sc53850, 1:50), or vimentin (Abcam, ab128507, 1:100) overnight at 4 °C. This was followed by incubation with secondary antibodies at 37 °C for 1 h. The nuclei were counterstained with 1 mg/ml DAPI (Sigma, D8417) for 2 min.

2.12 Toxicological experiments

2.12.1 Acute toxicity

For acute toxicity, HMTs on day 26, or 2D cultured Huh-7 were treated with a panel of hepatotoxins for 48 h. The compounds were chosen according to their known implications in DILI in humans based on the literature [18, 31]. For this purpose, 2D culture of 5×10^4 Huh-7 in DMEM were considered as control, and proper numbers of HMTs, containing equivalent numbers of Huh-7 cells, were transferred to ultra-low attachment plates. For drug exposure, culture media were replaced by serum-free media containing a certain concentration of each compound. Repeated 24 h dosing regime was carried out. Finally, the cell viability was assessed using MTS assay (Promega, Madison, WI, USA, G5421).

2.12.2 Dose- and time-dependency

To assess dose- and time-dependency, HMTs were treated with acetaminophen (APAP, Sigma-Aldrich, A7085), tamoxifen (TAM, Sigma-Aldrich, T5648), and fluorouracil (5-FU, Sigma-Aldrich, F6627) at three different concentrations, for 24, 48, and 72 h. Then, cell viability was evaluated using MTS assay. Treatments were started on day 21 and continued until measurements on day 24. Numbers of 2D cultured Huh-7 cells, as control, and HMTs were similar to those of the previous section.

2.13 Cytochrome P450 analysis

Basal CYP enzymes activity and their induction/inhibition were analyzed using P450-Glo Assay (Promega) kits according to lytic cell-based method, as described by the manufacturer. For this purpose, we used suggested kits for CYP3A4, 2C9, 2D6, and 2B6, and appropriate inducers or inhibitors (listed in Table S2). HMTs were exposed to inducers or inhibitors for 48 h. A Synergy HTX Multi-Mode Microplate Reader (Biotek) was used to analyze the luminescence of the resultant metabolites. Finally, the data obtained from induction or inhibition of CYP enzymes are presented as fold change, relative to its basal activity.

2.14 Statistical analysis

All quantitative data were analyzed using SPSS (v19.0) and graphs were prepared using GraphPad Prism (GraphPad Software, v6.0). Differences between the two groups were compared using two-tailed Student's t-test, and Analysis of variance (ANOVA) was used for comparison between more than two groups. All data are presented as means ± standard deviation (SD). *P*-values less than 0.05 were considered statistically significant.

3 Results

3.1 Characterization of composite hydrogel

In the current study, a biomimetic composite hydrogel was prepared, using LEM and alginate, in order to bioengineer hepatic micro-tissues. The LEM was prepared using a detergent washing and enzymatic digestion protocol (Fig S1A). The results of our previous study [28] confirmed that using this method, the major components of liver ECM, including collagens, laminin, fibronectin, and glycosaminoglycans (GAGs), were well preserved in the decellularized tissue while cells were effectively removed.

Upon neutralization (pH 7.4) and at 37 °C, the LEM solution comes into gelation via self-assembly of their fibrillar components such as collagen type I, allowing for cell encapsulation. However, the gelation is not quick enough and efficient to stabilize the LEMgel for scalable generation of HMTs. Furthermore, the LEMgel alone cannot sustain itself in the culture for a long time due to its low mechanical strength and degradation. To overcome this challenge, we have proposed a double-network composite hydrogel using a secondary network based on alginate, to allow fast gelation and support stability of the HMTs during the 28 days. In our study, when the generated HMTs fell into a gelling bath containing calcium chloride, a physical network is formed by rapid gelation of alginate which can work as a template for subsequent formation of the LEMgel network via self-assembly. Hence, the slow degradation of alginate network improves the stability of the double-network microcapsules during the one-month

culture. It is suggested that the composite hydrogel, with the tissue specificity of LEMgel and the physical nature of alginate, provide an appropriate micro-niche for cell encapsulation and scalable HMTs bioengineering. Evaluating ultrastructure using SEM analysis showed that the composite hydrogel is a highly porous network with interconnected micro-pores that could allow for efficient nutrition to support viability of the encapsulated cells (Fig S1B).

Prior to the generation of the double-network, we decided to assess the gelation ability of each physical network under appropriate physical conditions. The results showed prominent elastic behavior (G′ > > G″) and plateau behavior of the modulus versus frequency which are the signs of an efficient gel formation for both the LEM and alginate hydrogels (Fig S1C). The G′ mean value (Pa) was 117 for LEMgel, and 3383 for alginate. The higher modulus quantities of alginate hydrogel suggested higher crosslink density of this network as compared with LEM hydrogel; therefore, it could be a supportive scaffold for the weak network of LEMgel. As expected, the composite hydrogel showed an intermediate mechanical behavior (a mean G′ of 1215 Pa) compared to each hydrogel alone. This value is close to the value for liver ($\sim$ 1 kPa) [32].

3.2 Hepatic micro-tissue characterization

The HMTs were generated in three different diameters (300, 500, and 700 μm) by tuning air flow rate (between 0.8 and 1.4 bar) in an air-driven droplet generator system (Fig. 1A). Evaluating generated HMTs size distribution showed that the extrusion method could efficiently and reproducibly generate the HMTs with homogenous diameter (Fig. 1B, C). We found that the single cells were initially distributed homogeneously in the HMTs. While during the culture period, up to day 28, cell proliferation, aggregation or probably migration resulted in the formation of a number of cell aggregates inside the HMTs (Fig. 1B).

3.3 Hepatic micro-tissue size optimization

Generated HMTs of all three sizes maintained a uniform size with a non-significant little variation in diameter over the 28-days period of culture. However, the cell proliferation rate of three groups, calculated as fold change against the initial cell number, was different (Fig. 2A). On day 28, the cell fold-change of 300, 500, and 700 μm HMTs were 9.2 ± 0.3, 10.3 ± 0.4, and 6.9 ± 0.7, respectively, indicating significantly higher cell proliferation in HMTs with 500 μm diameter compared to other groups. In order to achieve the best size, we compared the three groups with regard to the improvement of hepatic-specific gene expression and function. In all groups, the highest mRNA

levels of fetal hepatocyte marker, alpha-fetoprotein (*AFP*), were observed on day 1, which declined over time (Fig. 2B), while mRNA levels of maturation markers, *ALB* and *CYP3A4*, were increased on days 14 and 28, in a manner that the expression level of these markers in 500 μm HMTs were significantly higher than those of other groups, particularly on day 28 ($p < 0.000$) (Fig. 2C). Furthermore, secretions of ALB on day 28, A1AT on days 21 and 28, and fibrinogen on days 1, 7, 14, 21 and 28, as well as urea production on day 21 were found to be significantly higher for 500 μm HMTs as compared those for 300 or 700 μm ones (Fig. 2D). Therefore, based on the data obtained, we selected 500 μm HMTs as the ones with optimum size for subsequent experiments. Using volumetric calculations and also cell counting by trypan blue, we found that there are about 490 cells in each 500 μm HMT on day 0. Therefore, it is expected that at this time, there are 245, 163, and 82, Huh-7, HUVECs, and MSCs, respectively, in one HMT.

3.4 Hepatic micro-tissues with 500 μm diameter, an appropriate *in vitro* liver model

3.4.1 Full characterization of HMTs

Live/Dead staining showed that most cells inside the HMTs were alive up to day 28, with only a small number of dead cells (Fig. 3A). To analyze the structure and glycogen storage, H&E and PAS staining were performed on HMTs sections. As expected and shown in phase-contrast micrographs, the sections revealed numbers of compact aggregating structures within one HMTs (Fig. 3B). Almost all Huh-7 cells had the ability to store glycogen in their cytoplasm and were PAS-positive (Fig. 3C). Furthermore, Huh-7 cells within the HMTs displayed typical functional features of mature hepatocytes, Dil-Ac-LDL intake, and ICG uptake/release (Fig. 3D, E). We further examined the expression of ALB and CYP3A4, as two important hepatic proteins, using immunofluorescence (IF) staining. The results demonstrated that the Huh-7 cell aggregates, which were organized within the HMTs, well expressed these proteins after 28 days of culture (Fig. 3F). Also, using IF staining against vimentin, we found that both MSCs and endothelial cells were organized in the HMTs in a close contact with Huh-7 cells (Fig. 3F).

Furthermore, we evaluated cell proliferation using IF staining and qRT-PCR to probe Ki-67 protein and mRNA expression in HMTs. The obtained data showed that many of cells were proliferating on day 14, but there was a significant decline in Ki-67 positive cells and gene expression on day 28 (Fig S2). Together, these data revealed that the proliferation and maturation of Huh-7 cells occurred in a sequential period.
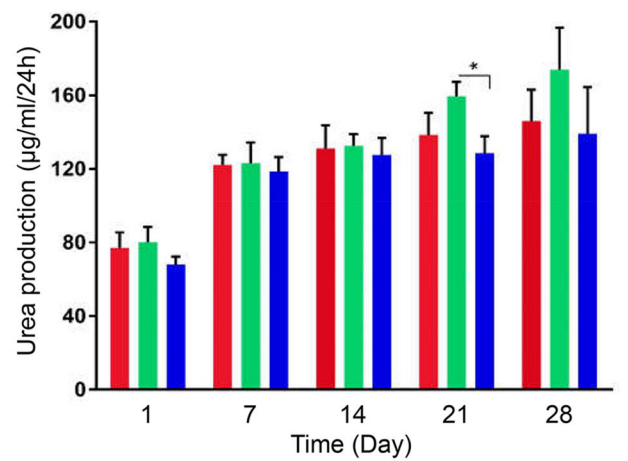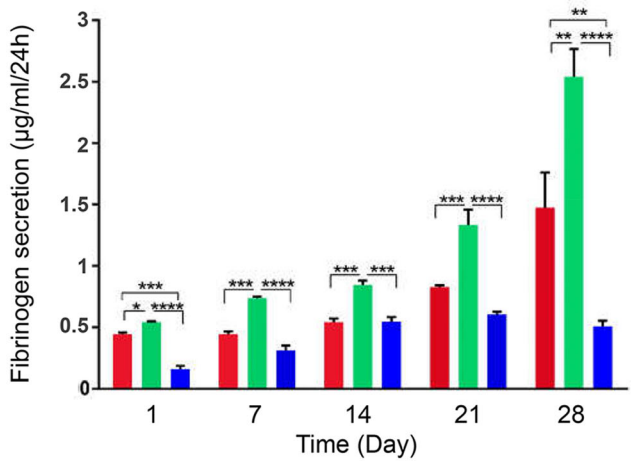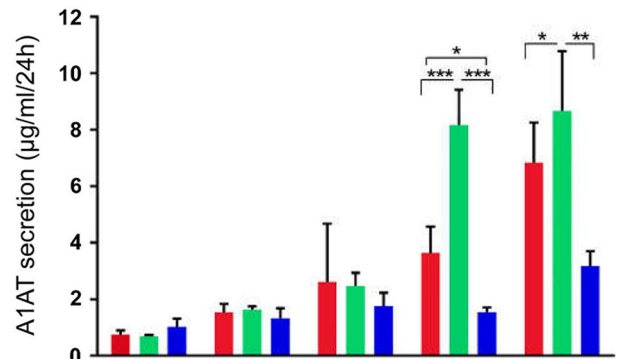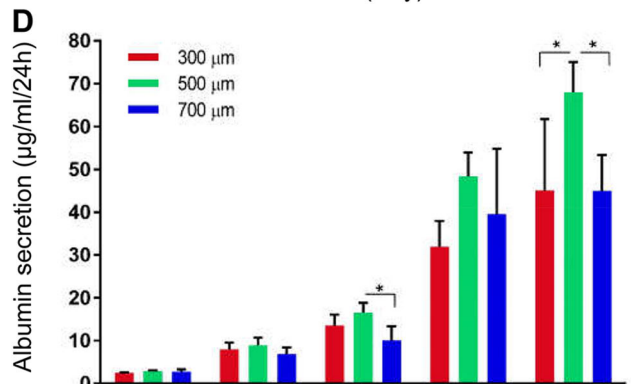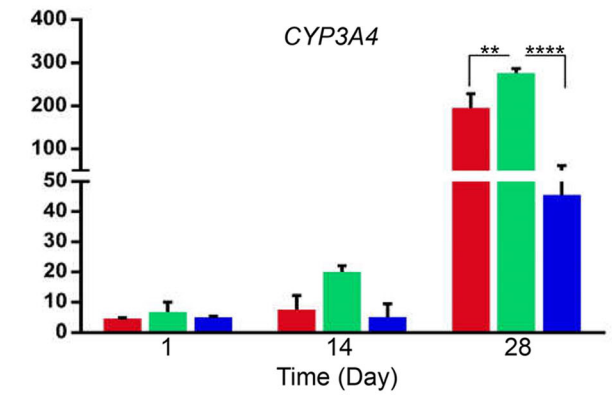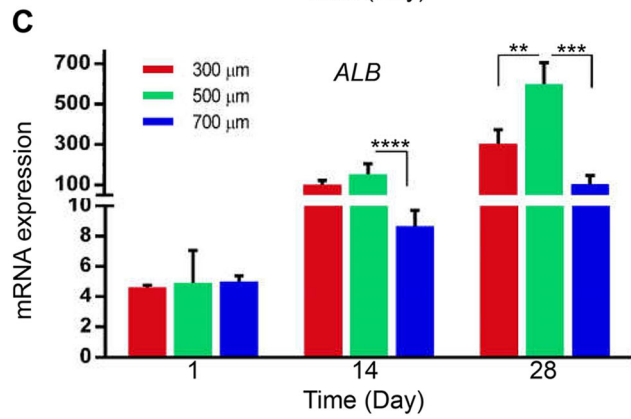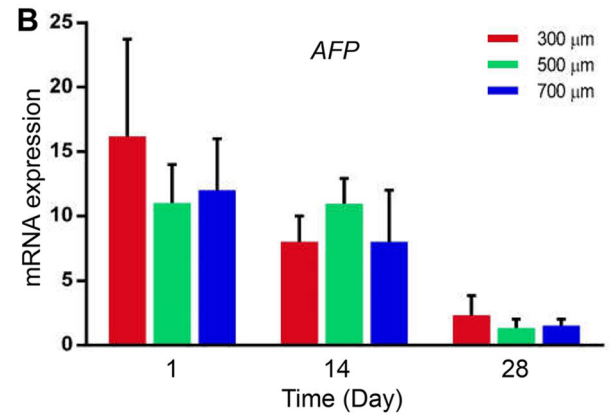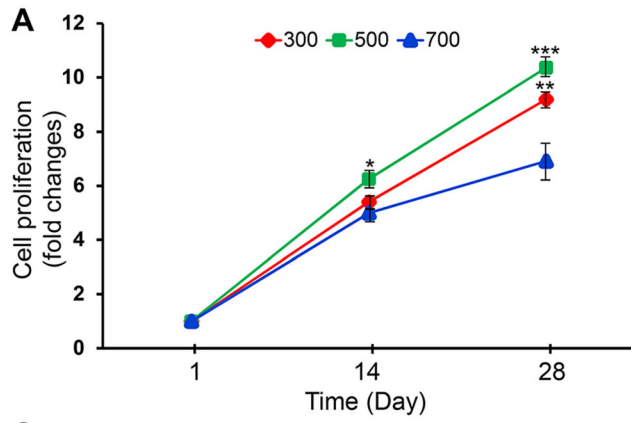
◀**Fig. 2** Comparison of 300, 500, and 700 μm hepatic micro-tissues made to choose the best size. **A** Cell proliferation rate during 28 days of culture showed that despite a little variation in HMTs diameter, cell proliferation rate of the HMTs with 500 μm diameter was significantly higher than other groups. **B, C** Gene expression of early (*AFP*) and late (*ALB* and *CYP3A4*) hepatic markers analyzed using qRT-PCR. The graphs demonstrated expression level of *AFP* declined throughout the time period. Notably, expression level of *ALB* and *CYP3A4*, particularly on day 28, was significantly higher in 500 μm HMTs compared to other groups. Data obtained were normalized against glyceraldehyde-3-phosphate dehydrogenase (GAPDH). **D** Secretions of ALB, A1AT, and fibrinogen as well as urea production were significantly higher for 500 μm HMTs compared with those of other groups. The data are presented as Mean ± SD (n = 3). *$p \leq 0.05$; **$p \leq 0.01$; ***$p \leq 0.001$; and ****$p \leq 0.0001$

3.4.2 Hepatic-specific genes expression

To determine whether the micro-niche provided in the selected HMTs (with 500 μm diameter) are suitable for improvement of Huh-7 cells functionality, expressions of a panel of hepatic-specific gene were analyzed using qRT-PCR during the culture period (Fig. 4). In the human liver, drugs are predominantly biotransformed by a subset of CYPs, namely CYP3A4, 1A2, 2B6, 2C9, 2C19, and 2D6 [33]. The gene expression analysis of these phase I enzymes illustrated significantly higher expression levels in HMTs, especially on day 28 ($p < 0.0001$) as compared with those of Huh-7 monolayer culture. We also found significant upregulation for nuclear pregnane X receptor (*PXR*), which is considered as one of the master regulators in drug metabolism [34], on days 14 and 28 in HMTs as compared with 2D cultured Huh-7. Multidrug resistance protein 2 (*MRP2*), as a transporter of drug metabolites, is an indicator for the formation of bile canalicular structures due to hepatocyte membrane polarity [35]. We found significantly higher expression level for MRP2 in the HMTs on day 28 as compared with 2D cultured Huh-7.

As illustrated in Fig. 4, mRNA levels of the hepatic functionality genes, carbamoyl phosphate synthetase-1 (CPS-1), and glucose 6-phosphatase (G6Pc), and transcription factor CCAAT/enhancer binding protein A (CEBPA) were significantly increased in HMTs in a time-dependent manner in comparison to those of 2D cultured Huh-7. Finally, the level of *ALB* expression in the HMTs on days 14 and 28 were 153 ± 51-fold and 600 ± 106-fold, respectively, which were higher than those of 2D cultured Huh-7.

In addition to gene expression, the secretion of four hepatic biomarkers, ALB, A1AT, fibrinogen, and urea, during the culture period was monitored. The results showed that the production of these hepatic biomarkers significantly increased over the period of 28 days in a time-

dependent manner in the HMTs as compared with those of 2D cultured Huh-7 (Fig S3).

3.4.3 Response to drug toxicity

After evaluations regarding functionality, to address our main purpose, we aimed to perform toxicological experiments including acute drug toxicity and dose- and time-dependency, as well as CYP enzymes evaluation.

Concentrations of some of the drugs were selected based on their therapeutic serum concentrations (C_{max}) and for others, we decided based on the literature [31]. For the acute drug toxicity, HMTs or 2D cultured Huh-7, as control, were exposed to an array of hepatotoxic compounds for 48 h. The results showed that with almost of the drugs, cell viability of the HMTs was lower than that of control group (Fig. 5). This reflected that the sensitivity and susceptibility of the HMTs to the hepatotoxins was higher than that of 2D cultured Huh-7 cells.

Paracetamol (APAP) is the most commonly used hepatotoxic drug in experimental models [36]. At the concentrations of 500 and 1000 μM, APAP caused a significant decrease in cell viability of HMTs as compared to the control group. Pioglitazone and ciglitazone are peroxisome proliferator-activated receptor (PPAR-γ) agonists. Ciglitazone has hepatotoxicity but pioglitazone is safe [37]. Regarding the specificity, in the current study, toxicities of these two structurally analogs were compared. Our results confirmed a more pronounced response to both components at 10 μM concentration in HMTs compared to the 2D cultured Huh-7 cells, as well as a higher susceptibility to ciglitazone compared with pioglitazone.

Dose- and time-dependency assay is one of the most mandatory processes in drug screening. So, we evaluated the dose- and time-dependency of three selected drugs, i.e. APAP, TAM, and 5-FU, for the HMTs (Fig. 6A). Our data confirmed that the HMTs, in most of the experiments, had proper sensitivity to increasing doses as well as increasing exposure times, which is expected from an appropriate *in vitro* model. We found that increasing doses (0.5, 1, and 10 mM) of APAP reduced cell viability following 24, 48, and 72 h of treatments. Compared to the untreated control, HMTs showed 68%, 63%, and 22% survival rates after 72 h exposure to APAP 0.5, 1, and 10 mM, respectively. Cell survival rate of HMTs correlated with TAM or 5-FU doses and exposure times, too. In this regard, the HMTs showed their sensitivity to both toxins in a time- and dose-dependent manner.

3.4.4 Cytochrome enzymes functionality

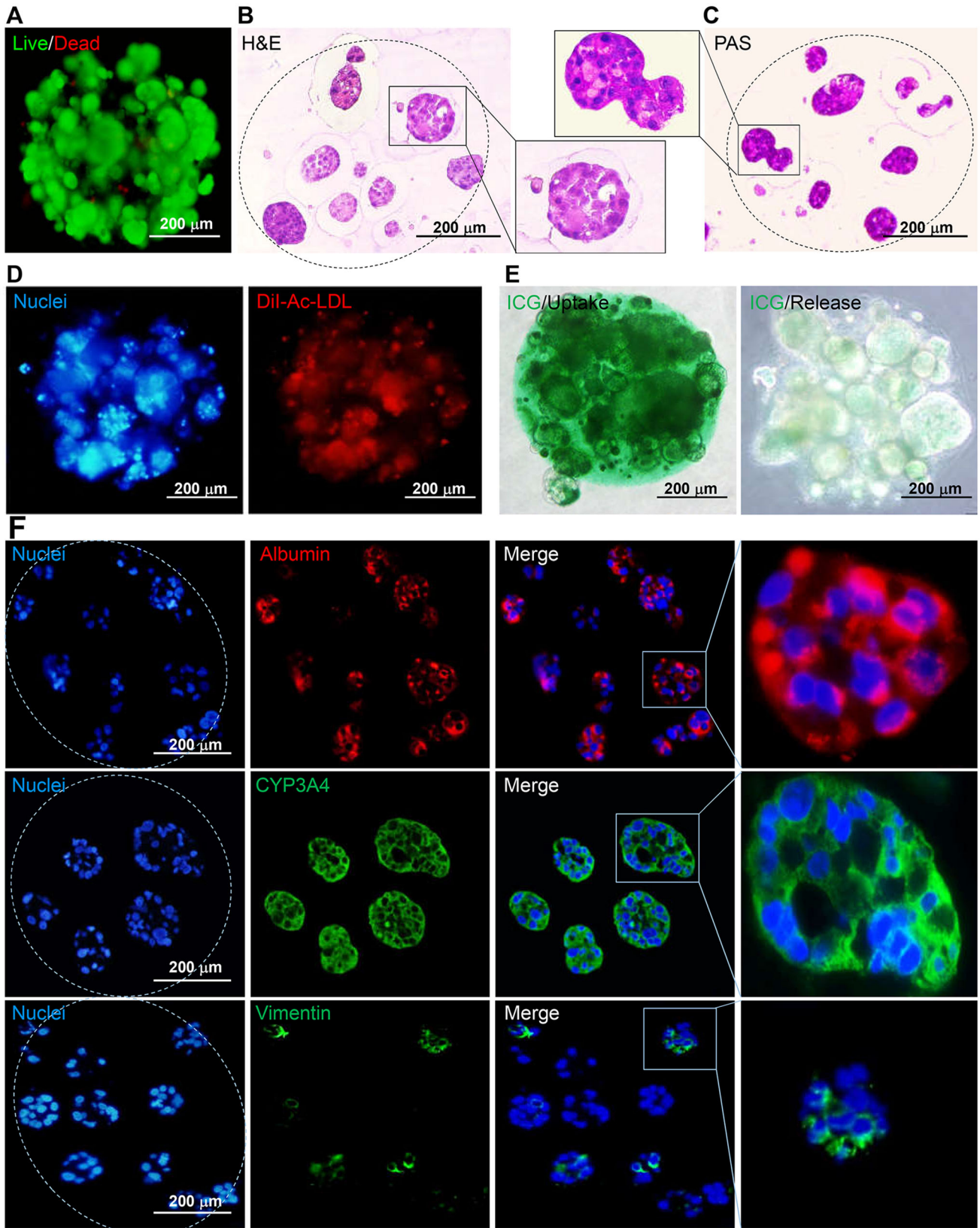One of the major determinant functional markers of hepatocytes, which extremely declined in the hepatoma cell

◀**Fig. 3** Further characterization of hepatic micro-tissues with 500 μm diameter. Micrographs of HMTs showed that on day 28 (**A**) most cells were alive and (**B**) a number of compact cell aggregates were formed within a HMT. Furthermore, almost Huh-7 cells displayed functional features typical of mature hepatocytes in terms of (**C**) epithelioid organization and glycogen storage, D) Dil-Ac-LDL intake, and (**E**) ICG uptake and release. (**F**) Immunofluorescence micrographs for ALB and CYP3A4 showed that the Huh-7 cell aggregates well expressed these proteins on day 28. Also, both MSCs and endothelial cells stained for vimentin were in a close contact with Huh-7 cells

lines, is the activity and induction/inhibition potency of the CYP450 enzymes [11]. To assess this fundamental capability, the HMTs, on day 21, were exposed to appropriate inducers or inhibitors for 48 h and the enzyme activity was reported as fold changes relative to non-exposed ones (Fig. 6B). For CYP3A4, the enzyme activity increased more than three folds when the HMTs were exposed to phenobarbital (PB), or a combination of PB and APAP, as inducers. Furthermore, CYP3A4 activity could be inhibited by verapamil, as a moderate inhibitor of the enzyme [38], where a threefold decrease in enzymatic activity was observed. Using PB or sodium valproate, as inducers, the activity of CYP2B6 showed more than twofold increase. However, we showed an inhibition of CYP2B6 by ciglitazone, a PPARγ agonist, although it was not found to be significant. For CYP2C9 induction, we used rifampicin (RIF), a PXR activator, or carbamazepine [39] and observed a two-fold elevation in the enzyme activity for rifampicin, while exposure to carbamazepine raised the enzyme activity non-significantly. Also, when CYP2C9 was inhibited by isoniazid, the enzyme activity was decreased significantly. Finally, the activity of CYP2D6 in the presence of rifampicin or dexamethasone (DEX) raised more than two-folds. Furthermore, the enzyme activity was inhibited four-folds, as compared with its basal activity, when the HMTs was exposed to diphenhydramine. These results showed that the induction/inhibition potency of CYP enzymes in the HMTs was acceptable according to the FDA guidelines (FDA). It can be stated that our satisfactory results from toxicological studies might have been obtained due to the improvement in the expression and activity of CYPs in the HMTs.

4 Discussion

A relevant *in vitro* liver model should possess a variety of criteria including allowing co-culture of hepatocytes with non-parenchymal cells in an appropriate micro-niche to remain functional for a long time in the culture. On the other hand, cost-effectiveness, feasibility, reproducibility, and compatibility for scalable production process are major

challenges. Numerous liver spheroid, micro-tissue or organoid models with considerable improvements in maintaining functionality of hepatocytes have been introduced. However, most of them require specialized equipment, are expensive, and/or not scalable. Due to these shortcomings, these *in vitro* models are not still implemented widely in drug development pipelines. In the present study, we developed a feasible, size controllable, reproducible and high-throughput compatible method for bioengineering functional hepatic micro-tissue, by co-culturing of Huh-7 cells with MSCs and HUVEC in a biomimetic composite hydrogel. All results obtained from the HMTs revealed significant improvements in hepatic-specific functionality and drug responsiveness compared to 2D cultured Huh-7.

One of the main issues regarding to *in vitro* liver models is the source of hepatocyte. PHHs, as the gold-standard for toxicity assay, are faced with lack of available sources and rapid dedifferentiation, which impede the use of these cells in drug discovery [12]. So, many researchers still have tried to predict the drug-induced cytotoxicity using hepatoma cell lines [5, 18, 21, 40]. Despite some advantages, such as lower price and reproducibility, using 2D cell line culture, 30% of the compounds were incorrectly classified as non-toxic [5]. It seems that improvement in the functions of cell lines may be an appropriate solution. The results of the previous studies have shown that 3D culture [21, 40], co-culture systems [19], the presence of ECM [16], or combining these parameters [28] may improve hepatic functionality of cell lines.

Supportive interactions from stromal cells enable hepatocytes to adopt a more tissue-like structure, which positively affect the cellular functionality [23, 24]. In the present study, similar to our previously reported data [28], we used two common, feasible, and accessible human cells, MSC and HUVEC, as supportive stromal cells for co-culturing with Huh-7. The heterotypic endothelial-hepatocyte interactions are important for hepatogenesis, hepatocellular polarity, and functionality, as well as liver regeneration [41, 42]. In a self-organizing liver bud and liver organoid generation, Takebe et al. showed that co-culturing of iPS-derived hepatocyte-like cells and HUVECs through paracrine signaling and especially cell–cell contact regulates hepatocyte differentiation and promotes the HLC maturation [43, 44]. Furthermore, Salerno et al. developed a liver organotypic co-culture systems using PHH and HUVEC and demonstrated that the cell–cell contact maintained functionality of hepatocyte during culture period [45]. Moreover, it is shown that, supported by endothelial cells, hepatocytes not only enhanced their primary metabolism, drug clearance, and gene expression but they also maintained a differentiated morphology and established a functional apico-basal polarization [46]. Furthermore, it is
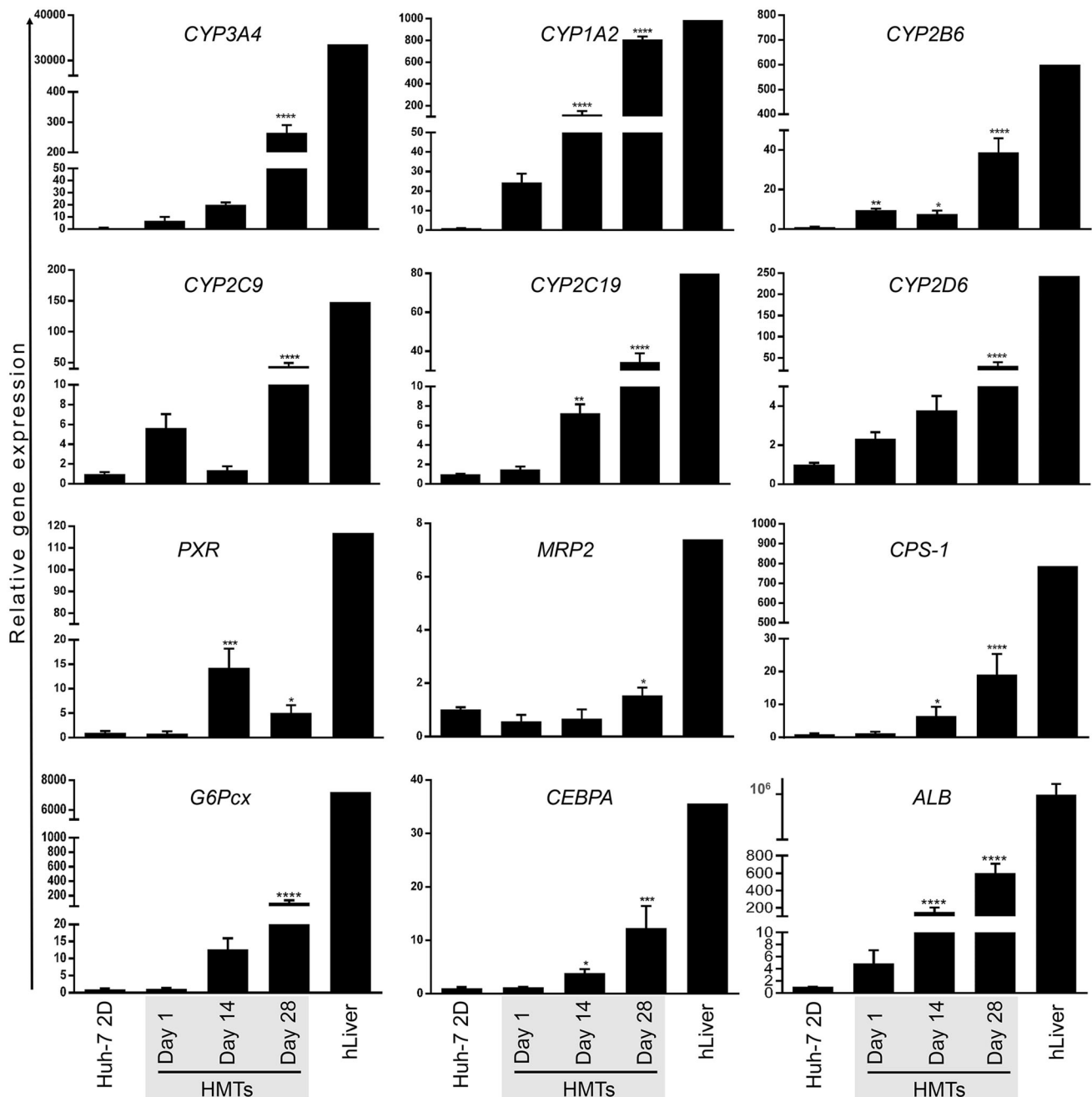
Fig. 4 Gene expression analysis of hepatic functionality markers for hepatic micro-tissues with 500 μm diameter. As demonstrated in the graphs, during the culture period, the majority of evaluated genes had significantly higher expression levels in the HMTs, especially on days 14 and 28 compared to Huh-7 monolayer culture. The mRNA expression levels were normalized against GAPDH and reported as fold changes relative to the expressions of 2D cultured Huh-7. The data are presented as Mean ± SD (n = 3). *$p \leq 0.05$; **$p \leq 0.01$; ***$p \leq 0.001$; and ****$p \leq 0.0001$

shown that co-culture of liver sinusoidal endothelial cells with primary rat hepatocytes in a layered model resulted in albumin expression maintenance up to day 37 [47]. Ma et al. used 3D bioprinting to create liver lobule-like structures containing hepatocyte-like cells, HUVECs, and adipose-derived stem cells embedded in a mixed GelMA and hyaluronic acid hydrogel. These hepatic hexagonal units were functional for up to 32 days, and the expression of liver-specific genes were at higher levels than in hepatocyte-like cells only group or monolayer culture [48]. In a liver micro-tissue model, which involves co-culture of HepaRG cell line and stellate cells, canalicular transporter MRP2 were functional, which might be due to higher levels of differentiation and polarization of hepatocytes [23].
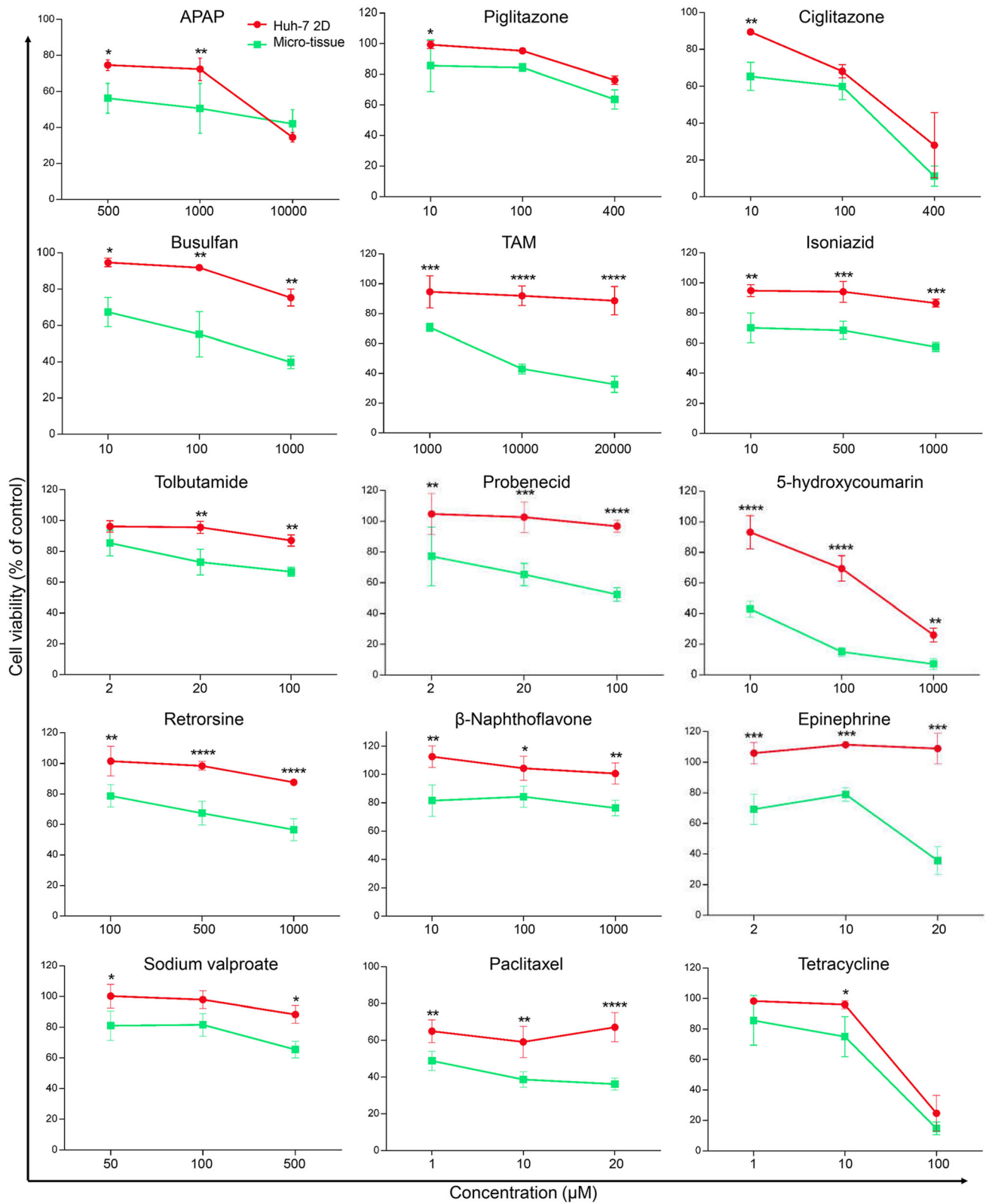
◄ **Fig. 5** Response of hepatic micro-tissues to acute toxicity. The response of the HMTs to hepatotoxins was assessed after 48 h exposure to different concentrations of a panel of 15 compounds. 2D cultured Huh-7 cells were considered for the control group and cell viability was evaluated using MTS assay and presented as the percentage of viable cells treated with chemical compound to ones treated by an appropriate vehicle. As shown in the graphs, in most of the experiments, the cell viability of HMTs was lower than that of the control group. This reflected that the susceptibility of the HMTs to most of the hepatotoxins was higher than that of 2D cultured Huh-7 cell. The data are presented as Mean ± SD (n = 3). *$p \leq 0.05$; **$p \leq 0.01$; ***$p \leq 0.001$; and ****$p \leq 0.0001$

As for the presence of ECM and its composition, scaffold-based *in vitro* models allow for more complex constructs that closely resemble the *in vivo* microenvironment. In a liver-on-a-chip spheroid-based model, where spheroids produced from HepG2/C3A cells encapsulated within GelMA hydrogel, ALB, A1AT, and transferrin values increased during 30 days [15]. In another study, Huh-7.5 cells grown on a fibronectin or collagen had higher ALB

expression at both gene and protein levels compared with without-ECM control group [16]. Recently, Lee et al. encapsulated hepatocyte-like cells using tissue-specific ECM microbeads to create uniform-sized tissue beads. The microbeads significantly enhanced the viability, maturation, and functionality of the cells, as compared with those of the collagen-only group [27]. Therefore, in the present study, we expected that a scaffold prepared based on tissue-specific ECM would provide enhancement of hepatocyte-specific functions of Huh-7 cells within the HMTs. As a major component of ECM, GAGs led to tissue-specific properties of ECM-derived biomaterials via sequestering tissue-specific growth factors and cytokines [49]. Furthermore, GAGs affect hepatic tissue reorganization through a variety of extracellular signaling [50]. Moreover, preserved fibronectin and collagen components in the natural ECM can mimic the liver microenvironment and improve hepatocyte viability and functionality by enhancing attachment and mechanical regulation [16].
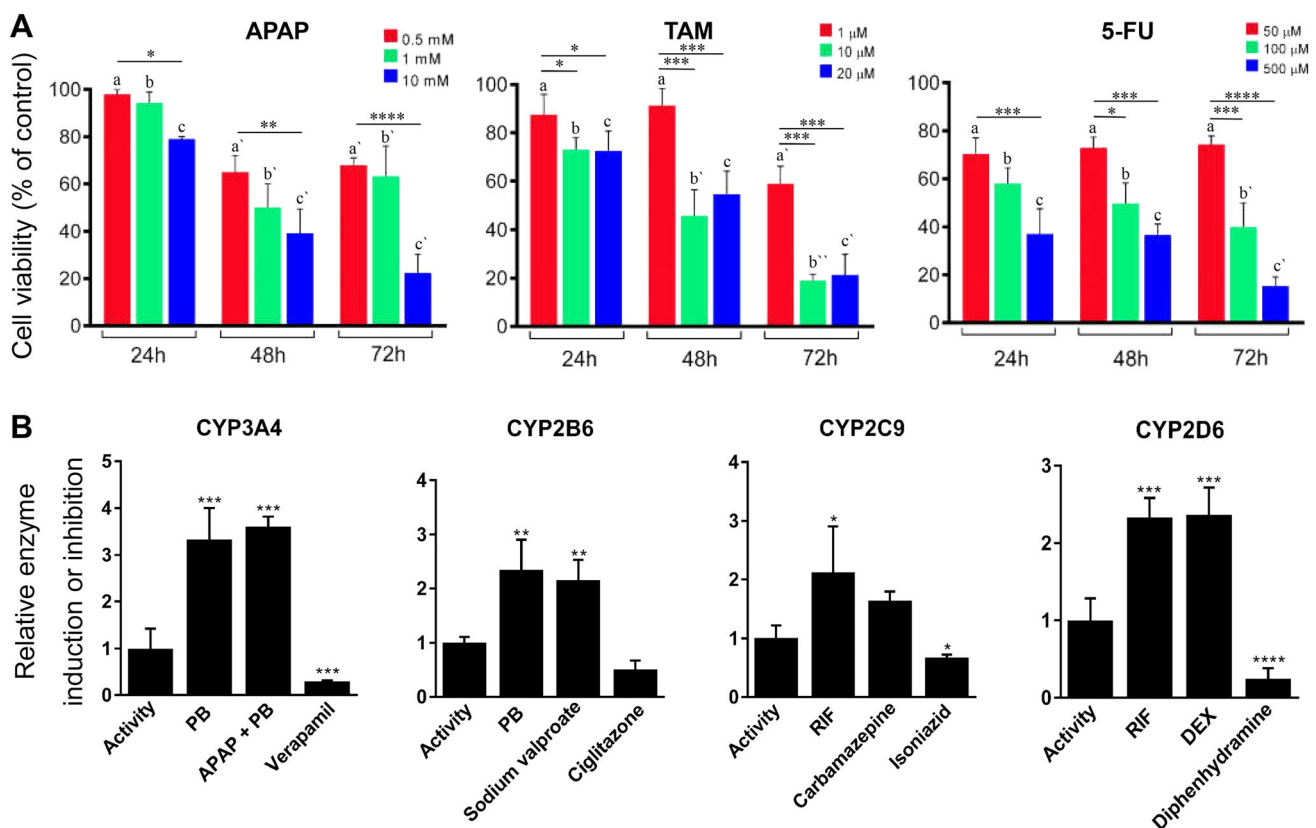

Fig. 6 Toxicological measurements for hepatic micro-tissues. **A** Assessments of responses to different doses and exposure periods of hepatotoxins showed that the HMTs, in most of the experiments, had proper sensitivity to increasing doses as well as increasing exposure times, which is expected from an appropriate *in vitro* model. **B** Measurements of CYP enzymes activity of the HMTs at steady state or after 48 h exposure to appropriate inducers or inhibitors showed acceptable induction and inhibition potency of the CYP enzymes compared with their basal activity. PB: phenobarbital; RIF: rifampicin; DEX: dexamethasone; APAP: acetaminophen. The data are presented as Mean ± SD (n = 3). *$p \leq 0.05$; **$p \leq 0.01$; ***$p \leq 0.001$; and ****$p \leq 0.0001$. Non-similar letters on the bars of same groups denote significant differences at $p < 0.05$

In addition to the biochemical properties of ECM, the stiffness of microenvironment is known to have significant effects on cellular behaviors [51]. Therefore, a niche at a physiological stiffness range can contribute more to bioengineering a more accurate hepatic model. Stiffness of our composite hydrogel was about 1.2 kPa, highly close to its value of the native liver matrix. It was previously shown that PHHs cultured on a substrate containing liver-specific ECM with 1.2 kPa stiffness demonstrated higher expression of hepatocyte nuclear factor 4 alpha (HNF4α) and ALB as compared to substrates with other stiffness values [52]. We used a double-network composite hydrogel which provided the tissue specificity of LEMgel and the physical nature of alginate, to allow fast gelation and provide the suitable stiffness to support the stability of the HMTs throughout the study.

Another key factor in 3D culture systems is to ensure that the recruiting scaffold is highly porous with interconnected channels to provide suitable cell attachment sites, to support cell spreading, proliferation, and formation of tissue-like structures and to enable efficient oxygen and nutrient supply, and waste removal [53, 54]. In this regard, some studies demonstrated that PLLA and alginate scaffold with pore size about 100 μm was optimum for culture, aggregate formation, and functionality of hepatocytes [55, 56]. Furthermore, our previous study showed a Hepatic-Patch generated by co-culture of human bone marrow stromal cells, HUVEC and Huh7, within a highly porous artificial 3D liver ECM scaffold improves liver-specific functionality of the hepatic cell line *in vitro* and *in vivo* [57]. In this study, the viability and improved functionality of HMTs proved that the composite hydrogel provides a suitable scaffold for generation of the hepatic micro-tissues.

In terms of cellular functionality, a circuit of gene expression, protein (enzyme) production, and the enzyme activity as well as its induction/inhibition capability are considerable. Successfully, in this regard, we could show such a phenomenon for some of the important hepatic-related functions, including ALB secretion, urea production, glycogen storage, and CYP enzyme activity involved in xenobiotic metabolisms. Our results showed that, compared to the control group, overexpression of *ALB* gene more than 600-times on day 28 in the HMTs leads to significantly more production of ALB. CPS-1, as the most abundant enzyme in hepatocyte mitochondria, catalyzes the rate-limiting step of the urea cycle. The elevated overexpression of *CPS-1*, more than 19-times, should be correlated with observed improvement in urea secretion of HMTs. G6Pc plays a key role in the connection between glycolysis, gluconeogenesis, glycogen synthesis, and glycogenolysis [58]. It suggests that the observed increase in *G6Pc* mRNA expression, i.e. more than 100-times,

might be in association with glycogen storage (PAS staining) in the HMTs.

One of the major determinant functional markers of hepatocytes is the activity and induction/inhibition potency of CYP450 enzymes [11]. Reduced expression of these enzymes in hepatoma cell lines is thought to be a main issue in the poor prediction of toxicity in humans [12]. To overcome this problem, the improvement in the functions of cell lines has been illustrated, which may lead to improved CYP activity [18]. Our results showed that not only the gene expression of all evaluated CYPs increased significantly, but the activity of the enzymes was also induced and inhibited by relative components. Furthermore, the activity of the CYP enzymes, as the most common phase I drug-metabolizing enzymes [33], were well demonstrated in our drug testing and toxicity experiments. In this regard, we used an array of experiments to test the effectiveness of the generated HMTs for drug toxicity assessment. In acute toxicity, HMTs were found to be more susceptible to hepatotoxins, indicated by less viability, compared with 2D cultured Huh-7. Furthermore, the response of the HMTs to selected hepatotoxins, APAP, TAM, and 5-FU, was dose- and time-dependent. Since the activity and inducibility of CYP enzymes are key factors of the drugs' pharmacokinetics and toxicity, the observed metabolic competence may improve the predictive power of the HMTs as an appropriate *in vitro* model.

Overall, although there is a great tendency to use PHHs or HLCs to develop *in vitro* human liver models, our data showed that cell lines might still be applicable when placed in a suitable microenvironment. Using this approach, the scalable bioengineered hepatic micro-tissues showed significant improvement in liver-specific functions especially in toxicological response and drug time- and dose-dependency.

Compliance with ethical standards

Conflict of interest The authors declare no conflicts of interest.

Ethical statement The study protocols and informed consents for human cells were approved by Medical Ethics Committee of Royan institute (IR.ACECR.ROYAN.REC.1396.250). In this regard, to obtain HUVECs from donated umbilical cords, informed consent was

obtained from the parents prior to the birth of healthy term neonates, in accord Journal of Biological Chemistry ance with the Declaration of Helsinki.

References

1. Watkins PB, Seeff LB. Drug-induced liver injury: summary of a single topic clinical research conference. Hepatology. 2006;43:618–31.
2. Materne EM, Tonevitsky AG, Marx U. Chip-based liver equivalents for toxicity testing–organotypicalness versus cost-efficient high throughput. Lab Chip. 2013;13:3481–95.
3. Hughes JP, Rees S, Kalindjian SB, Philpott KL. Principles of early drug discovery. Br J Pharmacol. 2011;162:1239–49.
4. Graham MJ, Lake BG. Induction of drug metabolism: species differences and toxicological relevance. Toxicology. 2008;254:184–91.
5. Kaplowitz N. Idiosyncratic drug hepatotoxicity. Nat Rev Drug Discov. 2005;4:489–99.
6. Hewitt NJ, Lechón MJ, Houston JB, Hallifax D, Brown HS, Maurel P, et al. Primary hepatocytes: current understanding of the regulation of metabolic enzymes and transporter proteins, and pharmaceutical practice for the use of hepatocytes in metabolism, enzyme induction, transporter, clearance, and hepatotoxicity studies. Drug Metab Rev. 2007;39:159–234.
7. Ware BR, Khetani SR. Engineered liver platforms for different phases of drug development. Trends Biotechnol. 2017;35:172–83.
8. Rowe C, Gerrard DT, Jenkins R, Berry A, Durkin K, Sundstrom L, et al. Proteome-wide analyses of human hepatocytes during differentiation and dedifferentiation. Hepatology. 2013;58:799–809.
9. Kiamehr M, Alexanova A, Viiri LE, Heiskanen L, Vihervaara T, Kauhanen D, et al. hiPSC-derived hepatocytes closely mimic the lipid profile of primary hepatocytes: a future personalised cell model for studying the lipid metabolism of the liver. J Cell Physiol. 2019;234:3744–61.
10. Takayama K, Kawabata K, Nagamoto Y, Kishimoto K, Tashiro K, Sakurai F, et al. 3D spheroid culture of hESC/hiPSC-derived hepatocyte-like cells for drug toxicity testing. Biomaterials. 2013;34:1781–9.
11. Schwartz RE, Fleming HE, Khetani SR, Bhatia SN. Pluripotent stem cell-derived hepatocyte-like cells. Biotechnol Adv. 2014;32:504–13.
12. Bhatia SN, Underhill GH, Zaret KS, Fox IJ. Cell and tissue engineering for liver disease. Sci Transl Med. 2014;6:245sr2.
13. Khetani SR, Berger DR, Ballinger KR, Davidson MD, Lin C, Ware BR. Microengineered liver tissues for drug testing. J Lab Autom. 2015;20:216–50.
14. Sison-Young RL, Mitsa D, Jenkins RE, Mottram D, Alexandre E, Richert L, et al. Comparative proteomic characterization of 4 human liver-derived single cell culture models reveals significant variation in the capacity for drug disposition, bioactivation, and detoxication. Toxicol Sci. 2015;147:412–24.
15. Bhise NS, Manoharan V, Massa S, Tamayol A, Ghaderi M, Miscuglio M, et al. A liver-on-a-chip platform with bioprinted hepatic spheroids. Biofabrication. 2016;8:014101.
16. Wang Y, Lee JH, Shirahama H, Seo J, Glenn JS, Cho NJ. Extracellular matrix functionalization and Huh-7.5 cell coculture promote the hepatic differentiation of human adipose-derived mesenchymal stem cells in a 3D ICC hydrogel scaffold. ACS Biomater Sci Eng. 2016;2:2255–65.
17. Tostões RM, Leite SB, Serra M, Jensen J, Björquist P, Carrondo MJ, et al. Human liver cell spheroids in extended perfusion bioreactor culture for repeated-dose drug testing. Hepatology. 2012;55:1227–36.
18. Ramaiahgari SC, den Braver MW, Herpers B, Terpstra V, Commandeur JN, van de Water B, et al. A 3D in vitro model of differentiated HepG2 cell spheroids with improved liver-like properties for repeated dose high-throughput toxicity studies. Arch Toxicol. 2014;88:1083–95.
19. Bell CC, Hendriks DF, Moro SM, Ellis E, Walsh J, Renblom A, et al. Characterization of primary human hepatocyte spheroids as a model system for drug-induced liver injury, liver function and disease. Sci Rep. 2016;6:25187.
20. Chang TT, Hughes-Fulford M. Monolayer and spheroid culture of human liver hepatocellular carcinoma cell line cells demonstrate distinct global gene expression patterns and functional phenotypes. Tissue Eng Part A. 2009;15:559–67.
21. Gaskell H, Sharma P, Colley HE, Murdoch C, Williams DP, Webb SD. Characterization of a functional C3A liver spheroid model. Toxicol Res (Camb). 2016;5:1053–65.
22. Sainz B Jr, TenCate V, Uprichard SL. Three-dimensional Huh7 cell culture system for the study of Hepatitis C virus infection. Virol J. 2009;6:103.
23. Wagner I, Materne EM, Brincker S, Süßbier U, Frädrich C, Busek M, et al. A dynamic multi-organ-chip for long-term cultivation and substance testing proven by 3D human liver and skin tissue co-culture. Lab Chip. 2013;13:3538–47.
24. Ramachandran SD, Schirmer K, Münst B, Heinz S, Ghafoory S, Wölfl S, et al. In vitro generation of functional liver organoid-like structures using adult human cells. PLoS One. 2015;10:e0139345.
25. Mobarra N, Soleimani M, Ghayour-Mobarhan M, Safarpour S, Ferns GA, Pakzad R, et al. Hybrid poly-l-lactic acid/poly (ε-caprolactone) nanofibrous scaffold can improve biochemical and molecular markers of human induced pluripotent stem cell-derived hepatocyte-like cells. J Cell Physiol. 2019;234:11247–55.
26. Ajoudanian M, Enomoto K, Tokunaga Y, Minami H, Chung S, Tanishita K, et al. Self-organization of hepatocyte morphogenesis depending on the size of collagen microbeads relative to hepatocytes. Biofabrication. 2019;11:035007.
27. Lee JS, Roh YH, Choi YS, Jin Y, Jeon EJ, Bong KW, et al. Tissue beads: tissue-specific extracellular matrix microbeads to potentiate reprogrammed cell-based therapy. Adv Funct Mater. 2019;29:1807803.
28. Saheli M, Sepantafar M, Pournasr B, Farzaneh Z, Vosough M, Piryaei A, et al. Three-dimensional liver-derived extracellular matrix hydrogel promotes liver organoids function. J Cell Biochem. 2018;119:4320–33.
29. Lotfinia M, Kadivar M, Piryaei A, Pournasr B, Sardari S, Sodeifi N, et al. Effect of secreted molecules of human embryonic stem cell-derived mesenchymal stem cells on acute hepatic failure model. Stem Cells Dev. 2016;25:1898–908.
30. Grässer U, Bubel M, Sossong D, Oberringer M, Pohlemann T, Metzger W. Dissociation of mono- and co-culture spheroids into single cells for subsequent flow cytometric analysis. Ann Anat. 2018;216:1–8.
31. Fey SJ, Wrzesinski K. Determination of drug toxicity using 3D spheroids constructed from an immortal human hepatocyte cell line. Toxicol Sci. 2012;127:403–11.
32. Kim HN, Kang DH, Kim MS, Jiao A, Kim DH, Suh KY. Patterning methods for polymers in cell and tissue engineering. Ann Biomed Eng. 2012;40:1339–55.
33. Rendic S, Guengerich FP. Survey of human oxidoreductases and cytochrome P450 enzymes involved in the metabolism of xenobiotic and natural chemicals. Chem Res Toxicol. 2015;28:38–42.

34. Küblbeck J, Jyrkkärinne J, Molnár F, Kuningas T, Patel J, Windshügel BR, et al. New in vitro tools to study human constitutive androstane receptor (CAR) biology: discovery and comparison of human CAR inverse agonists. Mol Pharm. 2011;8:2424–33.

35. Hoffmann U, Kroemer HK. The ABC transporters MDR1 and MRP2: multiple functions in disposition of xenobiotics and drug resistance. Drug Metab Rev. 2004;36:669–701.

36. McGill MR, Williams CD, Xie Y, Ramachandran A, Jaeschke H. Acetaminophen-induced liver injury in rats and mice: comparison of protein adducts, mitochondrial dysfunction, and oxidative stress in the mechanism of toxicity. Toxicol Appl Pharmacol. 2012;264:387–94.

37. Kostadinova R, Boess F, Applegate D, Suter L, Weiser T, Singer T, et al. A long-term three dimensional liver co-culture system for improved prediction of clinically relevant drug-induced hepatotoxicity. Toxicol Appl Pharmacol. 2013;268:1–16.

38. Martin P, Gillen M, Millson D, Oliver S, Brealey C, Grossbard EB, et al. Effects of CYP3A4 inhibitors ketoconazole and verapamil and the CYP3A4 inducer rifampicin on the pharmacokinetic parameters of fostamatinib: results from in vitro and phase I clinical studies. Drugs R D. 2016;16:81–92.

39. Lutz JD, Kirby BJ, Wang L, Song Q, Ling J, Massetto B, et al. Cytochrome P450 3A induction predicts p-glycoprotein induction; Part 2: prediction of decreased substrate exposure after rifabutin or carbamazepine. Clin Pharmacol Ther. 2018;104:1191–8.

40. Hurrell T, Lilley KS, Cromarty AD. Proteomic responses of HepG2 cell monolayers and 3D spheroids to selected hepatotoxins. Toxicol Lett. 2019;300:40–50.

41. Jung J, Zheng M, Goldfarb M, Zaret KS. Initiation of mammalian liver development from endoderm by fibroblast growth factors. Science. 1999;284:1998–2003.

42. Utley S, James D, Mavila N, Nguyen MV, Vendryes C, Salisbury SM, et al. Fibroblast growth factor signaling regulates the expansion of A6-expressing hepatocytes in association with AKT-dependent beta-catenin activation. J Hepatol. 2014;60:1002–9.

43. Takebe T, Sekine K, Enomura M, Koike H, Kimura M, Ogaeri T, et al. Vascularized and functional human liver from an iPSC-derived organ bud transplant. Nature. 2013;499:481–4.

44. Asai A, Aihara E, Watson C, Mourya R, Mizuochi T, Shivakumar P, et al. Paracrine signals regulate human liver organoid maturation from induced pluripotent stem cells. Development. 2017;144:1056–64.

45. Salerno S, Campana C, Morelli S, Drioli E, De Bartolo L. Human hepatocytes and endothelial cells in organotypic membrane systems. Biomaterials. 2011;32:8848–59.

46. Kidambi S, Yarmush RS, Novik E, Chao P, Yarmush ML, Nahmias Y. Oxygen-mediated enhancement of primary hepatocyte metabolism, functional polarization, gene expression, and drug clearance. Proc Natl Acad Sci U S A. 2009;106:15714–9.

47. Kang YBA, Rawat S, Cirillo J, Bouchard M, Noh HM. Layered long-term co-culture of hepatocytes and endothelial cells on a transwell membrane: toward engineering the liver sinusoid. Biofabrication. 2013;5:045008.

48. Ma X, Qu X, Zhu W, Li YS, Yuan S, Zhang H, et al. Deterministically patterned biomimetic human iPSC-derived hepatic model via rapid 3D bioprinting. Proc Natl Acad Sci U S A. 2016;113:2206–11.

49. Humphrey JD, Dufresne ER, Schwartz MA. Mechanotransduction and extracellular matrix homeostasis. Nat Rev Mol Cell Biol. 2014;15:802–12.

50. De Colli M, Massimi M, Barbetta A, Di Rosario BL, Nardecchia S, Devirgiliis LC, et al. A biomimetic porous hydrogel of gelatin and glycosaminoglycans cross-linked with transglutaminase and its application in the culture of hepatocytes. Biomed Mater. 2012;7:055005.

51. You J, Park SA, Shin DS, Patel D, Raghunathan VK, Kim M, et al. Characterizing the effects of heparin gel stiffness on function of primary hepatocytes. Tissue Eng Part A. 2013;19:2655–63.

52. Deegan DB, Zimmerman C, Skardal A, Atala A, Shupe TD. Stiffness of hyaluronic acid gels containing liver extracellular matrix supports human hepatocyte function and alters cell morphology. J Mech Behav Biomed Mater. 2016;55:87–103.

53. Mohanty S, Larsen LB, Trifol J, Szabo P, Burri HV, Canali C, et al. Fabrication of scalable and structured tissue engineering scaffolds using water dissolvable sacrificial 3D printed moulds. Mater Sci Eng C Mater Biol Appl. 2015;55:569–78.

54. Knight E, Przyborski S. Advances in 3D cell culture technologies enabling tissue-like structures to be created in vitro. J Anat. 2015;227:746–56.

55. Ranucci CS, Kumar A, Batra SP, Moghe PV. Control of hepatocyte function on collagen foams: sizing matrix pores toward selective induction of 2-D and 3-D cellular morphogenesis. Biomaterials. 2000;21:783–93.

56. Glicklis R, Merchuk JC, Cohen S. Modeling mass transfer in hepatocyte spheroids via cell viability, spheroid size, and hepatocellular functions. Biotechnol Bioeng. 2004;86:672–80.

57. Nobakht Lahrood F, Saheli M, Farzaneh Z, Taheri P, Dorraj M, Baharvand H, et al. Generation of transplantable three-dimensional hepatic-patch to improve the functionality of hepatic cells in vitro and in vivo. Stem Cells Dev. 2020;29:301–13.

58. Ghosh A, Shieh JJ, Pan CJ, Sun MS, Chou JY. The Catalytic Center of Glucose-6-phosphatase his176 is the nucleophile forming the phosphohistidine-enzyme intermediate during catalysis. J Biol Chem. 2002;277:32837–42.